Electronic Supplementary Material (ESI) for Journal of Materials Chemistry A.

Supporting Information

Nanoporous Cu@Cu_2O hybrid arrays enable photo-assisted supercapacitor with enhanced capacities

Cuihua An, Zhifeng Wang, Wei Xi, Kai Wang, Xizheng Liu,* Yi Ding*

Tianjin Key Laboratory of Advanced Functional Porous Materials, Institute for New Energy Materials & Low-Carbon Technologies, School of Materials Science and Engineering, Tianjin University of Technology, Tianjin 300384, P.R. China

*Corresponding author (email: xzliu@tjut.edu.cn; yding@tjut.edu.cn or yiding9312@126.com)

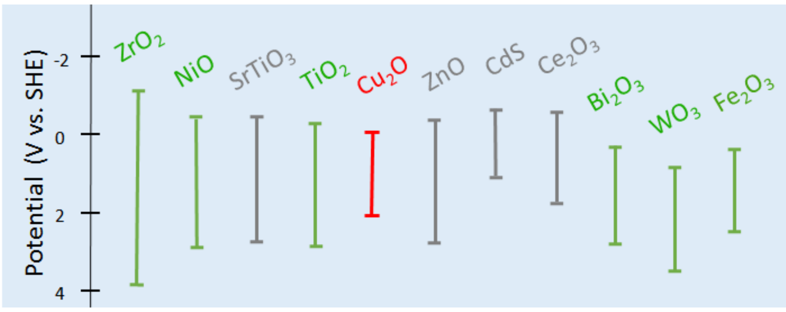

Fig. S1 The positions of the conduction band and the valence band for various semiconductor.

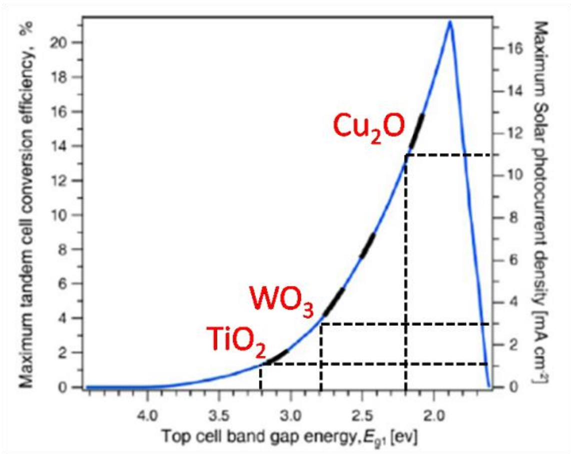

Fig. S2 Maximum solar-to-hydrogen conversion efficiency and solar photocurrent as a function of the band gap for commonly semiconductor oxide photoanodes.

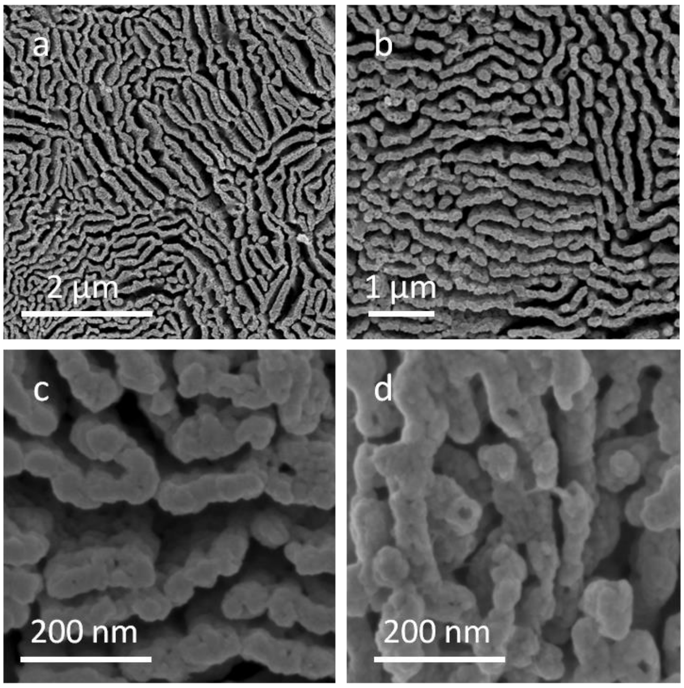

Fig. S3 SEM images of the top view (a-c) and cross section (b) of the NPC@Cu_2O composites.

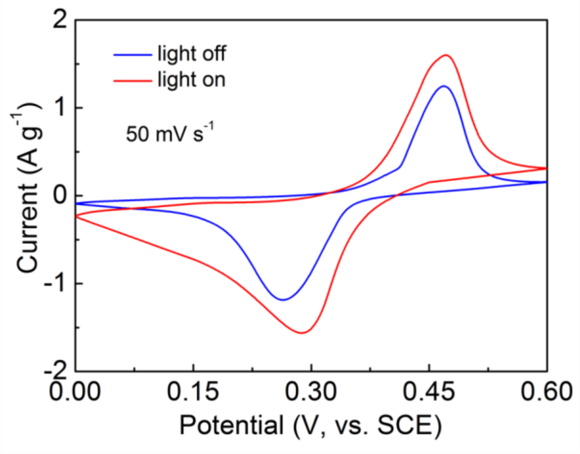

Fig. S4 CV curves of the NPC@Cu_2O electrode at 50 mV s^{-1} under dark condition and light illumination.

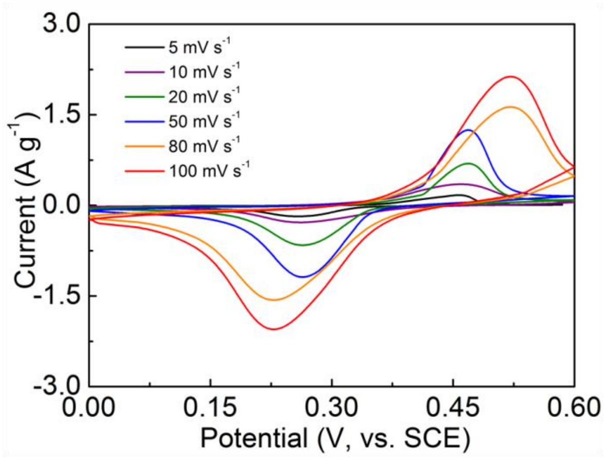

Fig. S5 CV curves of the NPC@Cu_2O electrode at various scan rates under dark condition.

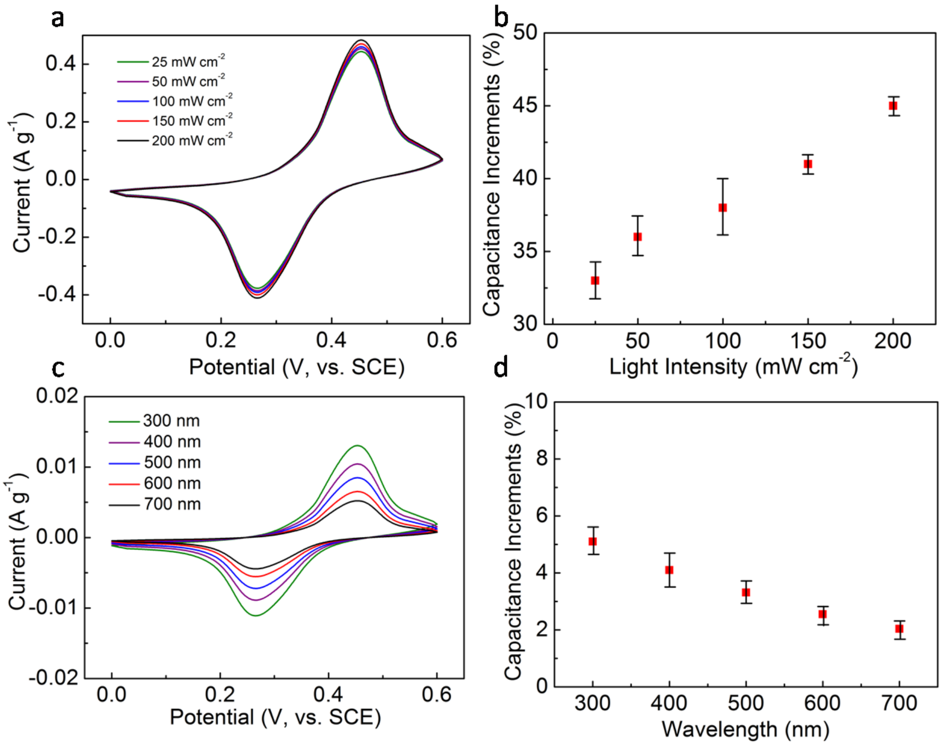

Fig. S6 CV curves of the NPC@Cu_2O electrode under different lighting intensities (a). Increments of capacitance achieved under different illumination intensities (b). CV curves of the NPC@Cu_2O electrode under light with various wavelengths (c). Increments of capacitance achieved under light with various wavelengths (d).

From Fig. S6a-b and Table S4, it can be clearly observed that the obtained capacitance increases from 658 to 718 F g^{-1} with increasing the illumination intensity from 25 to 200 mW cm^{-2}. For the precision, the parallel experiments were conducted to improve the quality of results. And the corresponding capacitance increment increases from 33 to 45% with increasing the illumination intensity. These results further confirm the impact of the light on the energy storage process.

In addition, the CV curves of the NPC@Cu_2O hybrid arrays under light with various wavelengths are depicted in Fig. S6c. As the wavelength decreases from 700 to 300 nm, the enclose areas of the CV curves and the peak current densities increase gradually. And the corresponding capacitance increment at various wavelengths decreases from 5.1 to 2.04 % (Fig. S6d). It is obvious that the increments dramatically increase when the wavelength is less than 500 nm, which is accordant with the CV curves.

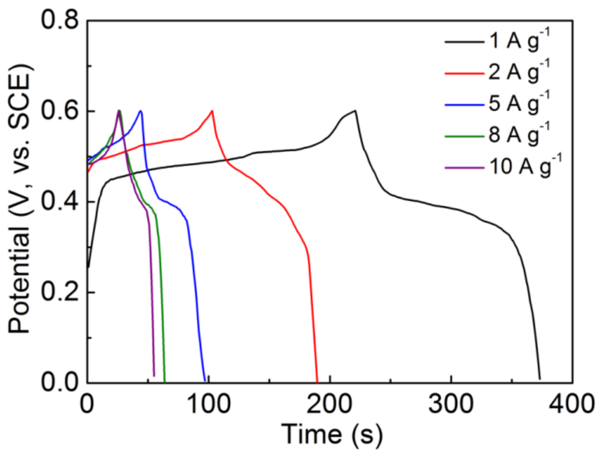

Fig. S7 Galvanostatic charge-discharge profiles at different current densities in dark condition.

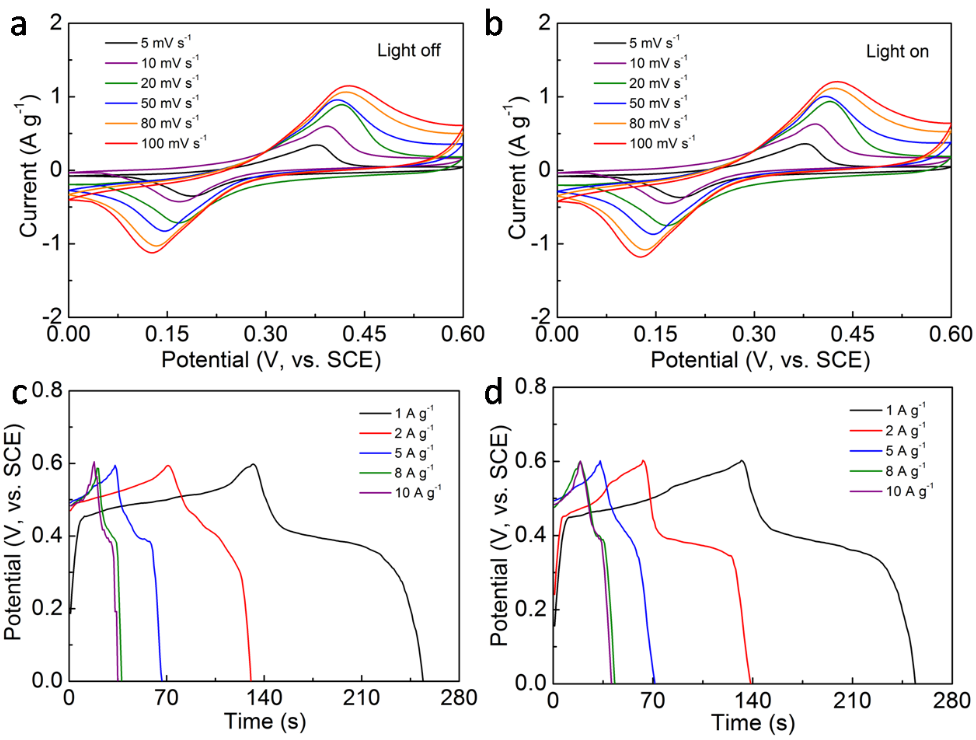

Fig. S8 CV curves of the Cu@Cu_2O electrode at various scan rates under dark condition (a) and light illumination (b). Galvanostatic charge-discharge profiles at different current densities under dark condition (c) and light illumination (d).

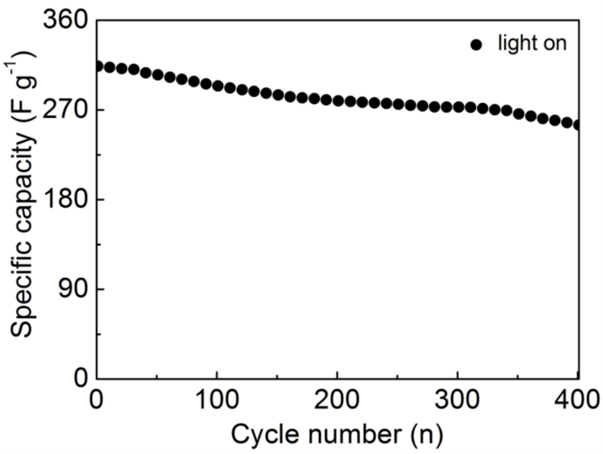

Fig. S9 The cycling stability of the NPC@Cu_2O electrode by charge/discharge measurement at 10 A g^{-1} under light illumination.

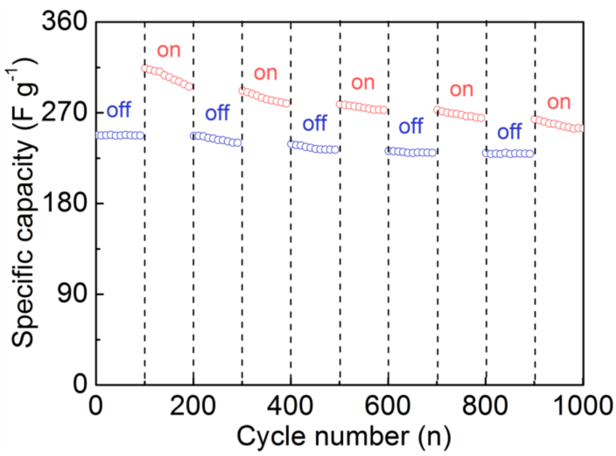

Fig. S10 The cycling stability of the NPC@Cu_2O electrode by charge/discharge measurement at 10 A g^{-1} under dark condition and light illumination.

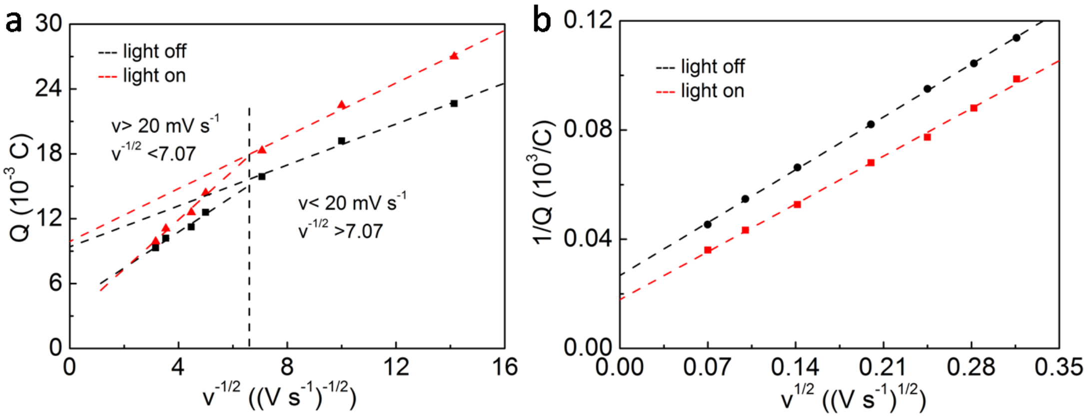

Fig. S11 The plot of charges versus $v^{-1/2}$ (a) and the plot of 1/Q versus $v^{1/2}$ (b) about the NPC@Cu_2O electrode in the dark and under light illumination.

In order to obtain the value of $Q_{surface}$ and Q_{pseudo}, the plot of Q versus $v^{-1/2}$ and the plot of 1/Q versus $v^{1/2}$ are drawn in Figure S11. Noted that only diffusion-controlled procedure is involved when the scan rate is infinite, $Q_{surface}$ can be calculated by extrapolating the plot with the y-axis (v>20 mV s^{-1} region) in Fig. S11a. The values of $Q_{surface}$ in dark condition and light illumination are 4.13×10^{-3} and 2.8×10^{-3} C, respectively. Similarly, when the scan rate is infinitesimal, the redox reaction dominates in storing energy so that the values of the Q_{pseudo} can be obtained. In Fig. S11b, Q_{pseudo} is y-intercept of the plots and the corresponding values are 37.39×10^{-3} and 55.86×10^{-3} C without and with illumination. Therefore, the capacitance increment under light illumination is primarily caused by the simulative pseudo-capacitive character.

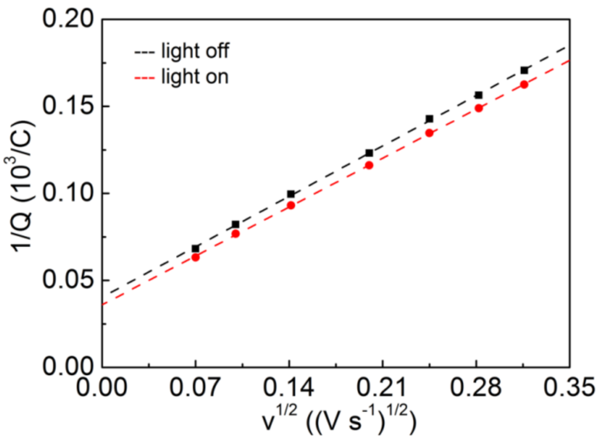

Fig. S12 The plot of 1/Q versus $v^{1/2}$ about the Cu@Cu_2O electrode in the dark and under light illumination.

Similarly, in Fig. S12, Q_{pseudo} values of the Cu@Cu_2O electrode are 25.25×10^{-3} and 27.62×10^{-3} C without and with illumination, far less than the NPC@Cu_2O electrode.

Table S1 EDS analysis results of the NPC sample

Element	Wt %	At %
Cu K	92.45	78.54
Al K	0.67	1.32
O K	6.88	20.14

Table S2 EDS analysis results of the NPC@Cu_2O hybrid

Element	Wt %	At %
Cu K	89.91	69.02
O K	10.09	30.98

Table S3 The capacitance of the NPC@Cu_2O electrode at various scan rates in dark condition

Scan rate (mV s^{-1})	5	10	20	50	80	100
Capacitance (F g^{-1})	511	495	421	326	271	220

Table S4 The capacitance of the NPC@Cu_2O electrode at different illumination intensities

Scan rate (mW cm^{-2})	25	50	100	150	200
Capacitance (F g^{-1})	658	673	683	698	718
Capacitance Increment (%)	33	36	38	41	45

Table S5 The capacitance at various current densities in dark condition

Scan rate (A g^{-1})	1	2	5	8	10
Capacitance (F g^{-1})	567	519	482	346	248

Table S6 The capacitance of the Cu@Cu_2O electrode at various scan rates

Scan rate (mV s^{-1})	5	10	20	50	80	100
Capacitance (F g^{-1}) without light	383	360	315	244	203	165
Capacitance (F g^{-1}) with light	413	381	330	251	208	168

Table S7 The capacitance of the Cu@Cu_2O electrode at various current densities

Scan rate (A g^{-1})	1	2	5	8	10
Capacitance (F g^{-1}) without light	442	404	361	270	193
Capacitance (F g^{-1}) with light	479	434	382	282	201